IEEE Photonics Journal
An IEEE Photonics Society Publication

Open Access

Metasurface Modeled as Chebyshev Impedance Transformer for Super-Broadband Anti-Reflection of Visible and Near Infrared Light

Volume 13, Number 3, June 2021

Byeong Je Jeon
Soo Jin Kim

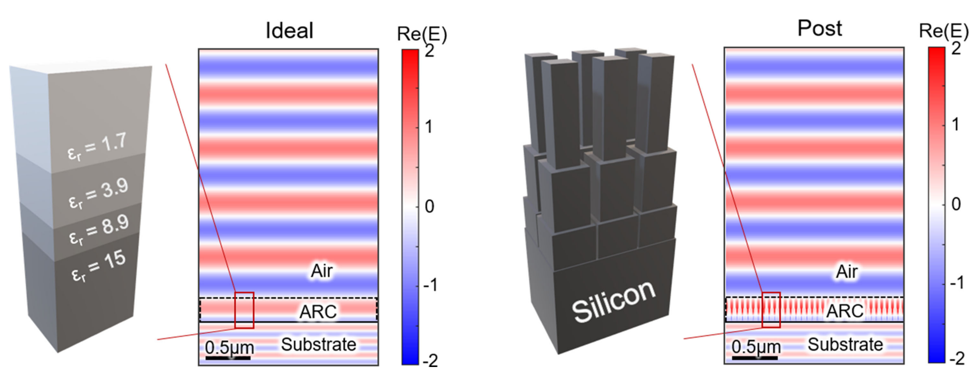

DOI: 10.1109/JPHOT.2021.3081728

Metasurface Modeled as Chebyshev Impedance Transformer for Super-Broadband Anti-Reflection of Visible and Near Infrared Light

Byeong Je Jeon and Soo Jin Kim

School of Electrical Engineering, Korea University, Seoul 02841, Republic of Korea

DOI:10.1109/JPHOT.2021.3081728

Manuscript received April 7, 2021; revised May 6, 2021; accepted May 15, 2021. Date of publication May 19, 2021; date of current version June 4, 2021. This work was supported in part by the National Research Foundation of Korea (NRF) under Grant NRF-2019R1C1C1004693, in part by the Samsung Electronics, and in part by the Samsung Research Funding & Incubation Center of Samsung Electronics under Grant SRFC-MA1901-03. Corresponding author: Soo Jin Kim (e-mail: kimsjku@korea.ac.kr).

Abstract: Facilitating anti-reflection has been of great scientific and practical interest due to its diverse applications in optical devices including solar cells and photodetectors. Various anti-reflection schemes are exploited and elaborated to realize effective broadband suppression of reflected light. In this work, we present and analyze a metasurface coating on silicon for efficient anti-reflection by leveraging the design rules of the Chebyshev transformer in the field of transmission line theory in the microwave regime. We explore the underlying physics of the metasurface by comparing the two representative types of constituent nanostructures and evaluating their optical properties using effective index retrieval methods. In particular, by designing nanostructures with subtle vertical etching in the pyramid valley, a broadband anti-reflection coating ranging from 400 to 1100 nm is achieved with reflection of less than 3%. We believe that the proposed design rule and analysis for this Chebyshev metasurface could pave an important way to realize systematic and effective anti-reflection schemes for diverse optical devices.

Index Terms: Metasurface, anti-reflection, Chebyshev transformer, subwavelength nanostructures.

1. Introduction

Reducing unwanted reflection has been of great scientific interest and practical importance for several decades in diverse fields such as transmission lines in microwaves [1], optical applications including solar cells, image sensors, and other light-absorbing devices [2]–[4]. A significant amount of research has been carried out to implement anti-reflection in such applications, especially to realize broadband and strong suppression of reflected waves. The conventional method to reduce reflection is implementing ultrathin layers with the thickness of quarter wavelength. By applying multi-stacking of such transforming layers with gradual changes in impedance that matches between the superstrate and substrate, it affords efficient and broadband control of the suppression of reflection. Examples of this include the Chebyshev and Binomial impedance matching transformers, and such approaches have been widely exploited and elaborated upon in transmission line theory in the microwave and terahertz regimes [5]. However, in the optical regime, such implementations are limited [6]–[8] since the optical properties of the materials are fixed and typically do not match with the arbitrarily determined impedances associated with the aforementioned impedance transformers. As such, there needs effective design strategy to realize anti-reflection in the visible spectrum akin to the well-established ones in the field of microwave and terahertz.

To realize broadband anti-reflection in the optical regime, a significant amount of research has been carried out by controlling scattering in structured surfaces and nanoparticles [9]–[12]. Such approaches effectively increase the optical path in forward propagating directions by inducing multiple bounces on the surfaces [13]–[15]. More recently, the nanophotonic approach has drawn much interest to realize anti-reflection by judiciously designing the metal and dielectric nanostructures that afford resonance [16]–[20]. For example, tuning of the multipole radiation of resonant nanoparticles leads to the effective forward scattering of light, known as the Kerker condition [21]–[23]. Moreover, strong light absorption in ultrathin nanostructured layers has been achieved based on the effect of plasmonics [24], [25] and dielectric resonances [26].

Here, we demonstrate an anti-reflection coating in the visible spectrum based on the model of Chebyshev impedance matching transformer by leveraging recent developments in metasurfaces. A metasurface is an ultrathin, structured film composed of nano-scatterers called meta-atoms that are arranged in subwavelength separations and feature the ability to arbitrarily control the optical properties of materials [27]–[29]. Since such an arrangement suppresses the excitation of higher diffraction order in the radiating far field, it behaves akin to a homogeneous film with a designer effective refractive index. Thus, there is a tantalizing opportunity to realize a metasurface which features the optimal impedance that matches the Chebyshev model for effective anti-reflection. Such an approach was originally proposed in several previous research. For example, in 1997, Philippe Lalanne and G Michael Morris described subwavelength surfaces of corrugated silicon which exhibit antireflection properties for visible light [30]. Such properties were analyzed based on the redistribution of energy and effective medium theory depending on the feature size of the corrugations. Numerous studies and models have been presented after the introduction of work by Lalanne et al. [31]–[33]. In this article, by leveraging the previous achievements and studies, we model a Chebyshev metasurface using silicon and carry out an in-depth analysis of the working principle of such metasurfaces, which has not been explored before. The core novelty is that we compare the underlying physics of two representative approaches, i.e., design of constituent nanostructures based on a nano-post or nano-mesh, and analyze the advantages of each approach based on effective medium theory. Specifically, we found the stark difference of optical phenomena between the mesh and post array by relating it with the one-dimensional array of corrugated lamellar structures. Next, we approximate the nanostructure as a pyramid shape to find the functional similarities. In particular, we find a unique design strategy for effective anti-reflection by showing that the etching of a subtle trench in the pyramid valley can substantially enhance the performance more than that of a typical pyramid structure [8].

2. Overview and Fundamentals

We start with a brief introduction to impedance matching transformers in transmission line theory and model it using nanostructured metasurfaces to apply it to the visible spectrum. A typical multi-section impedance matching transformer in transmission line theory [5] is composed of a load impedance Z_L and matching network Z_1 to Z_N with a characteristic impedance of $Z_n = \sqrt{\mu_n/\varepsilon_n}$. Broadband impedance matching can be achieved by stacking multiple impedances, where we denote the number of impedance matching layers as N. The matching network suppresses the reflectance caused by the difference between the load impedance and the characteristic impedance by designing the input impedance Z_{in} being equal to the characteristic impedance. To realize effective and broadband anti-reflection, two representative impedance matching models can be used. The first is the Binomial impedance matching transformer, and the other is the Chebyshev impedance matching transformer [5]. The former approach approximates the reflection coefficient

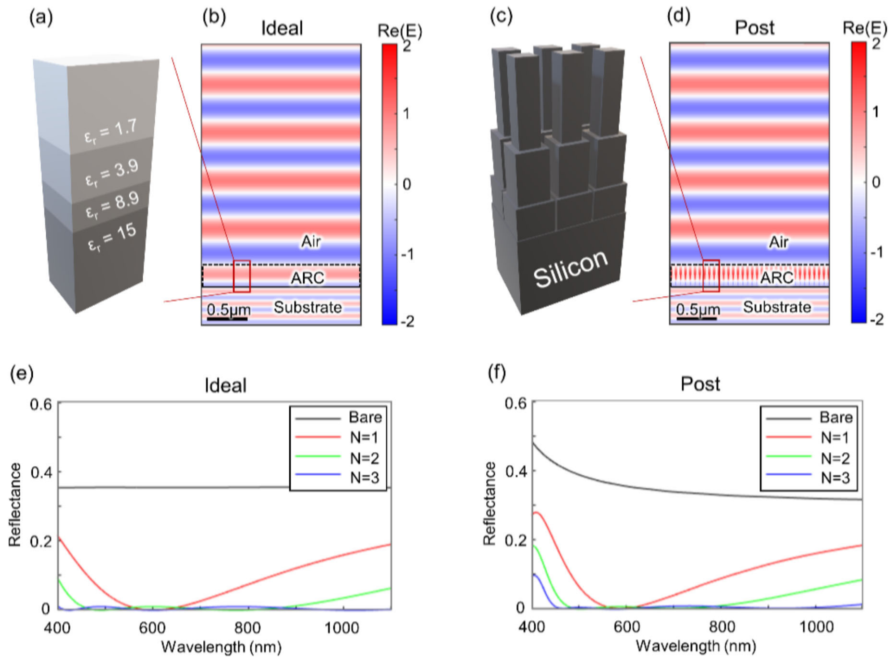

Fig. 1. Thin film and metasurface models that match Chebyshev impedance transformer center wavelength of 600 nm. (a) Schematic of an ideal transformer with three layers with optimized permittivities for anti-reflection coating (ARC). (b) Electric field profile with ideal ARC at a wavelength of 600 nm. (c) Schematic of a nanostructured metasurface that mimic the ideal Chebyshev anti-reflection transformer. (d) Electric field profile with a metasurface-based ARC at a wavelength of 600 nm. (e) Reflection spectrum $|\Gamma|^2$ of bare substrate with ε_r = 15.6 (black), Chebyshev ARC with a single layer (N = 1, red), two layers (N = 2, green) and three layers (N = 3, blue). (f) Reflection spectrum $|\Gamma|^2$ of bare silicon substrate (black), Chebyshev metasurface with a single layer (N = 1, red), two layers (N = 2, green) and three layers (N = 3, blue).

Γ to a binomial function and its reflectivity $|\Gamma|^2$ is maximally flat at the center frequency. The latter approach approximates the reflection coefficient to a Chebyshev polynomial and its reflectivity has ripples but a broader bandwidth than the former case [31]. Herein, we adopt the Chebyshev model to achieve more broadband suppression of reflected light than the maximum suppression at a specific wavelength, especially targeting the spectral range of visible and near-infrared wavelengths.

To realize Chebyshev matching to the silicon substrate ($\varepsilon_r =$ 15.6) in the visible spectrum, we model multi-layered thin films with optimized permittivities. As illustrated in Fig. 1(a), the matching network is converted to multi-layered films with each permittivity with $\varepsilon_n' + i\varepsilon_n''$. The load impedance is represented as a semi-infinite silicon substrate as a permittivity with $\varepsilon_s' + i\varepsilon_s''$. The reflection spectra of designed thin films are exhibited in Fig. 1(e), which shows the spectra of the Chebyshev model with the different number of layers ranging from one to three, i.e., N = 1, 2 and 3, where the corresponding curves are illustrated as red, green and blue lines, respectively. Note that the multi-layered films are designed to have a center wavelength being 600 nm, and the reflection spectrum of the bare substrate as a reference is exhibited as a black line. From the comparison, it is clearly observed that an increased in the number of matching layers results in more broadband suppression of reflected light.

To practically realize the optimized multi-layered films, we design a Chebyshev metasurface stack using silicon material. Carving the silicon film as a nanostructured metasurface could afford designer effective permittivity, and as such, the multi-layered metasurface could closely follow the properties of the ideal model of Fig. 1(a). The proposed metasurface is illustrated in Fig. 1(c) which consists of a square-cross-sectional shape of the nano-post array. By judiciously designing the filling ratio of the nano-post in each layer, we can effectively design the target permittivity and

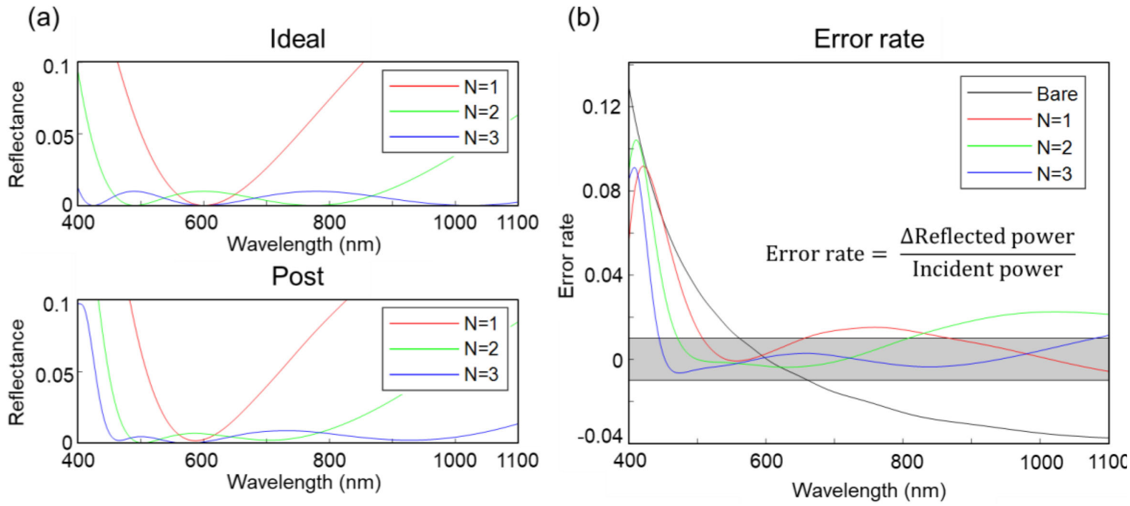

Fig. 2. Comparison between the ideal model and the metasurface consisting of nanopost array. (a) Reflection spectra $|\Gamma|^2$ of Chebyshev ARC with ideal thin film model (top) and nanopost-based metasurface model (bottom). (b) The error rate of nanopost model with respect to the ideal model. The error rate is defined as Error rate = ΔReflected_power/Incident_power, whose value is just equal to the difference of the reflectance.

corresponding impedance values. To compare the metasurface with the ideal multi-layered model, the profiles of the electric field are visualized using finite difference time domain simulations as exhibited in Fig. 1(b) and (d). From the panels, it is clearly observed that the two examples show the identical phase and amplitude of the electric field in both air and substrate side implying that the nanostructured metasurface functions akin to the optimized Chebyshev layers. The quantitative reflection spectrum (Fig. 1(f)) closely follows the spectrum of the ideal layers (Fig. 1(e)), and as the number of nanostructured layers increases, the spectrum is more broadly suppressed.

We further analyze how the material's dispersion influences the design of Chebyshev model compared to the ideal multi-layered films with constant refractive index. The reflection spectra of the two models are shown in Fig. 2. Note that the reflections are plotted up to 10% for clear comparison and visualization, which exhibits the trend in the number and position of dips as the number of layers increases. To quantitatively analyze the broadband anti-reflection characteristics of the metasurface model compared to the ideal one, we define error rate as the ratio of the difference of reflectance (ΔReflected_power) to incident power (Fig. 2(b)). The overall error rate decreases as the number of layers increases, which becomes less than 1% in the wavelength range of 450 nm to 1100 nm when the number of layers being equal to three ($N = 3$). In the following discussion, we prove that such alleviation of error rate in metasurfaces is related to the strong field concentration in the air gap region in nanopost array, which results in a significantly reduced effect by the material's dispersion (blue line) compared to the effect in the planar surface (black line).

3. Design and Analysis

3.1 Nano-post and Nano-Mesh Array

As a next stage, we carry out in-depth analysis of the designed metasurfaces by numerically extracting the effective permittivity of two representative types of constituent nanostructures. From the rest of the analysis, we choose the number of layers being equal to three ($N = 3$) which achieves a reasonable level of broadband suppression of reflected light. To achieve optimal performance

TABLE 1

Optimal Values of Permittivity and Dimension in Each of the Three Coating Layers for the Ideal Chebyshev transformer. A Target Wavelength of 600 nm and $|\Gamma_m| = 0.1$ are Chosen for Chebyshev Method Calculation for Efficient Anti-Reflection Over the Spectral Range of 400 – 1100 nm

Target layer	Thickness (nm)	Relative permittivity, ε_r	Filling Fraction
1st layer	d_1=114	1.7	Post 0.89 Mesh 0.67
2nd layer	d_2=76	3.9	Post 0.61 Mesh 0.31
3rd layer	d_3=50	8.9	Post 0.25 Mesh 0.09

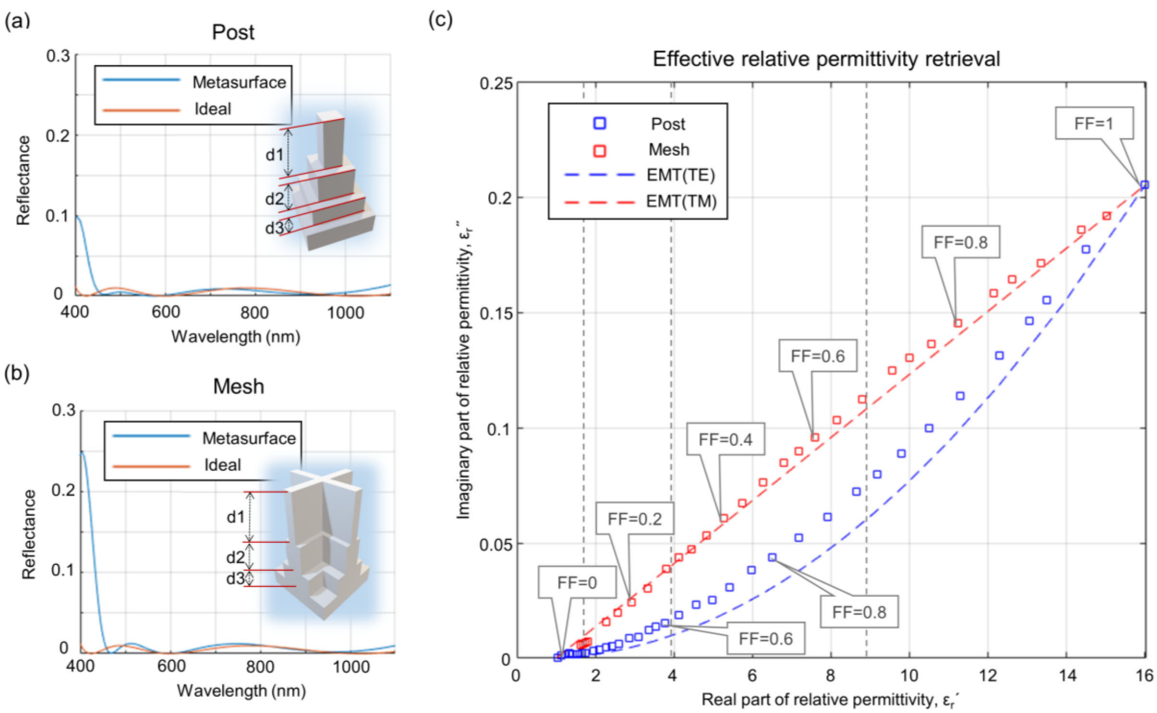

Fig. 3. Analysis of Chebyshev metasurfaces with meta-atoms composed of a nano-post or nano-mesh array based on the effective electromagnetic parameter retrieval method. (a) Reflection spectra of the nano-post-based metasurface (blue) and ideal model (red). (b) Reflection spectra of the nano-mesh-based metasurface (blue) and ideal model (red). (c) The retrieved effective permittivities for nano-post (blue rectangles), nano-mesh (red rectangles) for diverse filling ratios (FFs) of the nanostructure. The values are extracted by designing a single nanostructured layer. The values closely match the theoretical permittivities based on the effective medium theory (EMT) of the one-dimensional array of a lamellar structure under polarization parallel to the axis (TM, red dashed line) and perpendicular to the axis (TE, blue dashed line).

over the spectrum ranging from 400 to 1100 nm, the permittivity and thickness of each layer is theoretically obtained based on the Chebyshev method as exhibited in Table 1 [5], [31].

The permittivity gradually increases and the thickness of the film gradually decreases as each layer is close to the bottom silicon substrate as shown in Table 1. To realize the Chebyshev matching layers using metasurfaces, two representative types of nanostructure, i.e., nano-post and nano-mesh array, are designed by changing the filling fraction of each layer as illustrated in the schematics in Fig. 3(a) and (b). Here, the filling fraction (FF) is defined as $FF = Area_{structure}/Area_{unit\ cell}$ whose value changes from 0 to 1. The period of the unit cell is set to 60 nm, which is the subwavelength scale, to support only zeroth diffraction order by preventing opening of higher diffraction channels. The designed nanostructures show effective suppression of reflection akin to the homogeneous Chebyshev layers, as observed in the spectra in Fig. 3 (a) and (b), which compare the ideal model (red line) with the metasurface (blue line) consisting of either a nano-post or nano-mesh array. While there are slight mismatches between the two models near the wavelength of 400 nm owing to the nontrivial rise in the intrinsic refractive index of silicon near the ultraviolet regime, the overall trends of anti-reflection are similar, with three ripples of suppression near the target wavelengths.

The optimized nanostructures are systematically designed by retrieving the effective permittivities of metasurfaces that match the values in Table 1. Fig. 3(c) shows the effective permittivities of the proposed nanostructures for various FF ranging from 0 to 1. The blue and red rectangles indicate the retrieved values for the nano-post and nano-mesh respectively. The values are obtained by extracting the S-parameter from the amplitude and phase of reflected and transmitted light [34]. The three vertical black dotted lines are the optimal permittivities of the ideal Chebyshev model. Note that we mainly focus on the matching of the real part of permittivity, which dominantly determines the performance of the Chebyshev model. Choosing an optimal FF that matches the ideal Chebyshev values affords effective anti-reflection in a broad spectral range.

3.2 Effective Medium Theory

More intriguing than the high performance is the insight into the matching mechanisms of the proposed nanostructures. It is found from the retrieved values that there is a stark difference in matching impedance~~s~~ between the nano-post and nano-mesh structures in Fig. 3(c). Interestingly, the nano-post and nano-mesh which feature rotationally symmetric geometry show permittivity values that are close to the effective permittivity of anisotropic lamellar structures, i.e., a one-dimensional array of nanobeams [35]. The theoretical effective permittivities of a lamellar structure under the polarization of incident light perpendicular to the axis (TE) and parallel to the axis (TM) are represented by the blue and red dotted lines in Fig 3(c), respectively. The curves are calculated based on the first-order effective medium theory (EMT) as [30], [35], [36]

$$\hat{\varepsilon}_{\mathrm{eff,TE}} = \left(\frac{f_1}{\hat{\varepsilon}_1} + \frac{f_2}{\hat{\varepsilon}_2}\right)^{-1}, \tag{1}$$

$$\hat{\varepsilon}_{\mathrm{eff,TM}} = f_1\,\hat{\varepsilon}_1 + f_2\hat{\varepsilon}_2, \tag{2}$$

where $\hat{\varepsilon}_1$ and $\hat{\varepsilon}_2$ are the permittivities of air and the nanostructure, and f_1 and f_2 are the volume fraction of each medium, i.e., $f_1 + f_2 = 1$. It is clearly observed that these two curves closely overlap with the simulated values of the nano-post and nano-mesh arrays. This can be explained by the similarity in underlying physics between the features of the anisotropic lamellar structure and the proposed rotational symmetric structures. In the case of the nano-post array (Fig. 4(a)), the electric field is concentrated outside of the structures, as illustrated in Fig. 4(b) and (c), which is observed in the case of a lamellar structure under TE polarization due to the continuity of electric flux in the normal direction to the index boundary [37]. Thus, the effective permittivity of the nano-post array follows the EMT curve of TE polarization. On the other hand, in the case of the nano-mesh array (Fig. 4(d)), the electric field is strongly concentrated into the nanostructures. It is clearly observed in Fig. 4(e) and (f) that the electric field is strongly and selectively concentrated along the nanobeams directed parallel to the direction of polarization and is depleted in the nanobeams directed perpendicular to the polarization. Thus, the nano-mesh array operates for any polarization very similar to a one-dimensional array of wires under TM polarization [37]. From the analysis, it is concluded that while both of the two different types of designs achieve Chebyshev anti-reflection, their underlying physics closely follow the EMT of anisotropic one-dimensional arrays with specific polarizations.

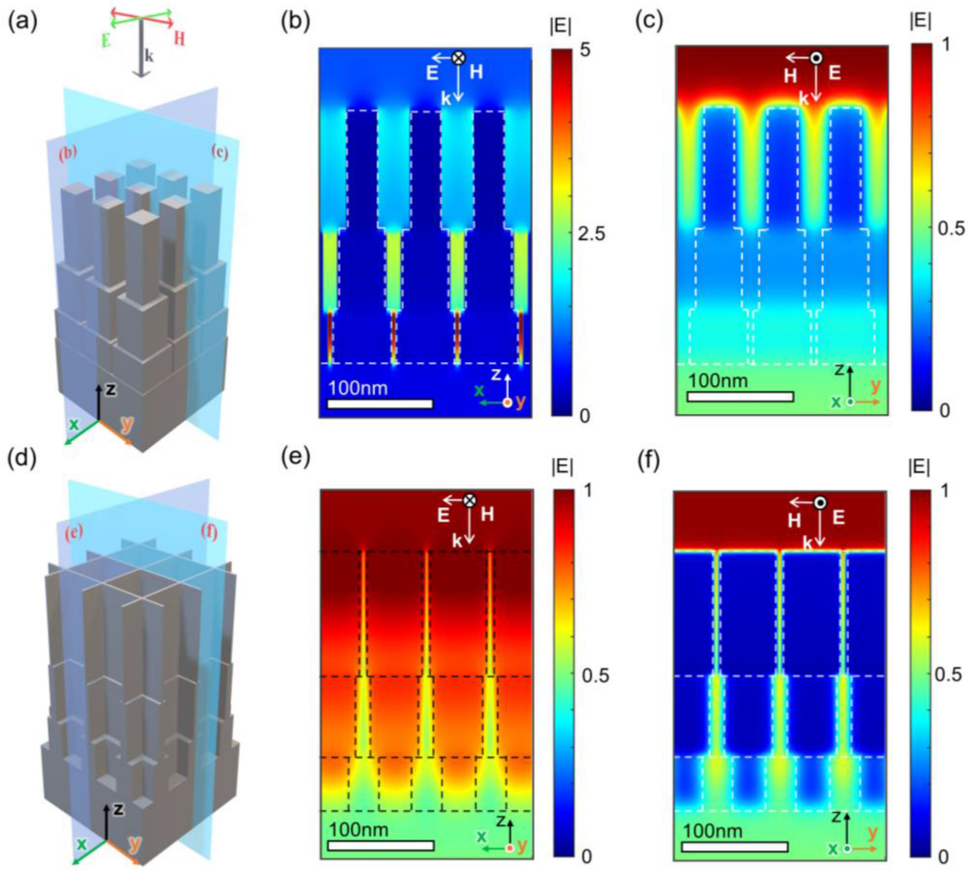

Fig 4. The profile of electric field for nano-post and nano-mesh structures. Schematic of the nano-post array (a) with the electric field along the plane directed parallel to the polarization (b) and perpendicular to the polarization (c). The field is concentrated outside of the nanostructures akin to the one-dimensional array with TE polarization. Schematic of the nano-mesh array (d) with the plane parallel to the polarization (e) and perpendicular to the polarization (f). The field is concentrated into the nanostructures akin to the one-dimensional array with TM polarization.

3.3 Nano-pyramid Array

Finally, we approximate the proposed nano-post array as a pyramid structure to reduce the structural complexity. More importantly, we find that inducing additional, subtle etching at the valley of the pyramid array could significantly enhance anti-reflection akin to the optimized nano-post array. Fig. 5 shows the evolved steps to design broadband anti-reflection coating. Based on the nano-post array as a reference structure (Fig. 5(a) to (c)), the pyramid array in Fig. 5(d) is designed with the same period and height. The side slope of the pyramid is chosen in a manner that the difference between each volumetric portion of the pyramid and the corresponding nano-post layer is at a minimum. It is noteworthy that the pyramid array has a slightly different reflection spectrum, i.e., there is an overall increase in reflection in the near-infrared region, compared to the spectrum of the nano-post array. This stems from the discrepancy in the ability to concentrate the electric field at the very narrow air gaps in the bottom Chebyshev layer, whereas the optical profiles of the upper region in both cases show close similarities (Fig. 5(b, c) and (e, f)). To overcome this limitation, we further design the pyramid array by subtle etching in the valley of the pyramid to realize the third Chebyshev layer, as shown in Fig. 5(g). It is found from this minor variation that the newly designed structure facilitates broadband antireflection over the wavelength range of 400 to 1100 nm with three minimum ripples akin to the stair-shaped, three-layered Chebyshev metasurface.

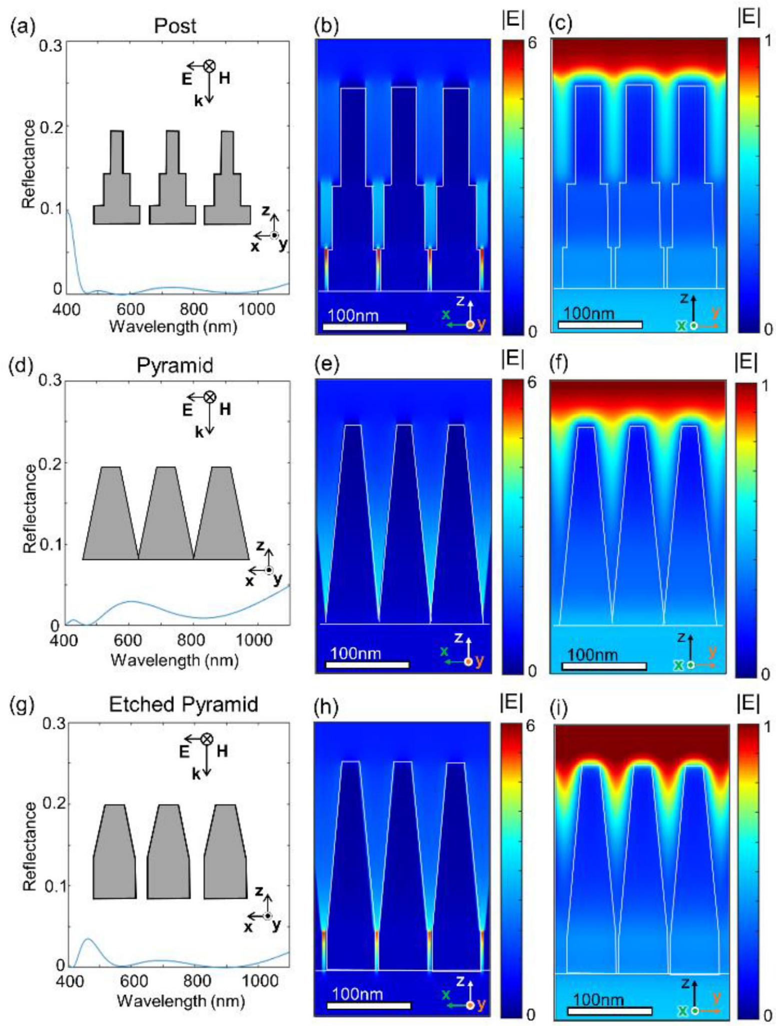

Fig. 5. Design of Chebyshev metasurfaces with a three-step nanopost array (a-c), nano-pyramid array (d-f) and nano-pyramid with additional etching in the valley (g-i). The reflection spectrum of the etched pyramid (g) features close to the spectrum of the nano-post array (a), the profiles of the electric field show similarities between the two structures.

This fact implies that the additional, precise design near the substrate to concentrate field plays a crucial role in realizing more efficient suppression of reflection in the broader spectral regime without excessively high aspect ratio of nanocones (Fig. 5(h, i)).

In Addition, we further propose a potential fabrication process of the designed structure. The etched pyramid array which is suggested for experimental approximation can be fabricated by the suggested steps as illustrated in Fig. 6. The processes including the Langmuir-Blodgett method [38], Self-ordering dewetting [39]–[41], and Metal-assisted chemical etching (MACE) [42] have been extensively developed and matured which are applicable to fabricating the structures. Also, since the combination of such processes can be adopted independently in the aspect of chemical and physical effect, we believe that the optimization of suggested fabrication steps can effectively realize the presented nanostructured array.

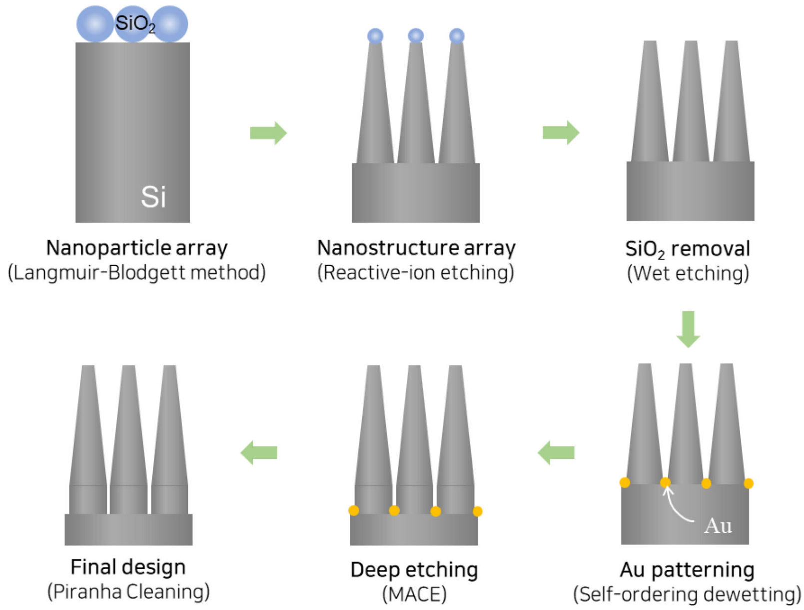

Fig. 6. A fabrication process for the proposed design. After placing the nanoparticle array through the Langmuir-Blodgett method, the nanostructure arrays are formed by the Reactive-ion etching (RIE) process. Then the Au atoms are patterned using Self-ordering dewetting or Templated dewetting, and the final design is realized using Metal-assisted chemical etching (MACE).

4. Conclusion

To summarize, multi-layered Chebyshev metasurfaces were presented based on subwavelength nanostructures including nano-post, nano-mesh and pyramid arrays. An in-depth analysis was carried out to understand the underlying physics in modeling the metasurfaces by comparing them with the conventional effective medium theory of the one-dimensional array with anisotropic geometry. Furthermore, by optimizing the pyramid structure to effectively mimic the Chebyshev model, we achieved a broadband anti-reflection coating ranging from 400 to 1100 nm, which is the spectrum for the silicon materials to absorb light. We believe that the proposed design and the analysis pave an important pathway for realizing ultrathin Chebyshev metasurface schemes for systematic and effective anti-reflection platforms.

References

[1] H. F. Pues and A. R. Van De Capelle, “An impedance-matching technique for increasing the bandwidth of microstrip antennas,” *IEEE Trans. Antennas Propag.*, vol. 37, no. 11, pp. 1345–1354, Nov. 1989.
[2] M. W. P. E. Lamers *et al.*, “17.9% Metal-wrap-through mc-Si cells resulting in module efficiency of 17.0%,” *Prog. Photovolt. Res. Appl.*, vol. 20, no. 1, pp. 62–73, 2012.
[3] W. H. Southwell, “Pyramid-array surface-relief structures producing antireflection index matching on optical surfaces,” *J. Opt. Soc. Amer. A*, vol. 8, no. 3, pp. 549–553, 1991.
[4] P. Spinelli, M. Hebbink, R. De Waele, L. Black, F. Lenzmann, and A. Polman, “Optical impedance matching using coupled plasmonic nanoparticle arrays,” *Nano Lett.*, vol. 11, no. 4, pp. 1760–1765, 2011.
[5] D. M. Pozar, *Microwave Engineering*. Hoboken, NJ, USA: Wiley, 2011.
[6] J. Zhao and M. A. Green, “Optimized antireflection coatings for high-efficiency silicon solar cells,” *IEEE Trans. Electron Devices*, vol. 38, no. 8, pp. 1925–1934, Aug. 1991.
[7] S. Chhajed, M. F. Schubert, J. K. Kim, and E. F. Schubert, “Nanostructured multilayer graded-index antireflection coating for si solar cells with broadband and omnidirectional characteristics,” *Appl. Phys. Lett.*, vol. 93, no. 25, 2008, Art. no. 251108.
[8] J. Zhu *et al.*, “Optical absorption enhancement in amorphous silicon nanowire and nanocone arrays,” *Nano Lett.*, vol. 9, no. 1, pp. 279–282, 2009.
[9] P. Campbell and M. A. Green, “Light trapping properties of pyramidally textured surfaces,” *J. Appl. Phys.*, vol. 62, no. 1, pp. 243–249, 1987.

[10] K. Nakayama, K. Tanabe, and H. A. Atwater, "Plasmonic nanoparticle enhanced light absorption in GaAs solar cells," *Appl. Phys. Lett.*, vol. 93, no. 12, 2008, Art. no. 121904.
[11] J. Van De Groep, P. Spinelli, and A. Polman, "Single-step soft-imprinted large-area nanopatterned antireflection coating," *Nano Lett.,* vol. 15, no. 6, pp. 4223–4228, 2015.
[12] H. A. Atwater and A. Polman, "Plasmonics for improved photovoltaic devices," *Nat. Mater.*, vol. 9, no. 3, pp. 205–213, 2010.
[13] E. Yablonovitch and G. D. Cody, "Intensity enhancement in textured optical sheets for solar cells," *IEEE Trans. Electron Devices*, vol. 29, no. 2, pp. 300–305, Feb. 1982.
[14] E. Yablonovitch, "Statistical ray optics," *J. Opt. Soc. Amer.*, vol. 72, no. 7, pp. 899–907, 1982.
[15] P. B. Clapham and M. C. Hutley, "Reduction of lens reflexion by the 'Moth eye' principle," *Nature*, vol. 244, no. 5414, pp. 281–282, 1973.
[16] L. Cao *et al.*, "Semiconductor nanowire optical antenna solar absorbers," *Nano Lett.,* vol. 10, no. 2, pp. 439–445, 2010.
[17] A. I. Kuznetsov, A. E. Miroshnichenko, M. L. Brongersma, Y. S. Kivshar, and B. Luk'yanchuk, "Optically resonant dielectric nanostructures," *Science*, vol. 354, no. 6314, 2016, Art. no. 846.
[18] C. F. Bohren, and D. R. Huffman, *Absorption Scattering Light by Small Particles*. Hoboken, NJ, USA: Wiley, 1998.
[19] A. M. Shaltout, J. Kim, A. Boltasseva, V. M. Shalaev, and A. V. Kildishev, "Ultrathin and multicolour optical cavities with embedded metasurfaces," *Nat. Commun.*, vol. 9, no. 1, 2018, Art. no. 2673.
[20] J. Park, S. J. Kim, and M. L. Brongersma, "Condition for unity absorption in an ultrathin and highly lossy film in a Gires–Tournois interferometer configuration," *Opt. Lett.*, vol. 40, no. 9, pp. 1960–1963, 2015.
[21] J. van de Groep, and A. Polman, "Designing dielectric resonators on substrates: Combining magnetic and electric resonances," *Opt. Exp.*, vol. 21, no. 22, pp. 26285–26302, 2013.
[22] A. Pors, S. K. H. Andersen, and S. I. Bozhevolnyi, "Unidirectional scattering by nanoparticles near substrates: Generalized Kerker conditions," *Opt. Exp.*, vol. 23, no. 22, pp. 28808–28828, 2015.
[23] W. Liu, and Y. S. Kivshar, "Generalized Kerker effects in nanophotonics and meta-optics," *Opt. Exp.*, vol. 26, no. 10, pp. 13085–13105, 2018.
[24] J. Park, J. H. Kang, X. Liu, and M. L. Brongersma, "Electrically tunable epsilon-near-zero (ENZ) metafilm absorbers," *Sci. Rep.*, vol. 5, 2015, Art. no. 15754.
[25] C. Zhang, Q. Qian, L. Qin, X. Zhu, C. Wang, and X. Li, "Broadband light harvesting for highly efficient hot-electron application based on conformal metallic nanorod arrays," *ACS Photon.*, vol. 5, no. 12, pp. 5079–5085, 2018.
[26] W. Zhu *et al.*, "Wideband visible-light absorption in an ultrathin silicon nanostructure," *Opt. Exp.*, vol. 25, no. 5, pp. 5781–5786, 2017.
[27] Q. Chen *et al.*, "Nanowire-based ultra-wideband absorber for visible and ultraviolet light," *Opt. Laser Technol.*, vol. 105, pp. 102–105, 2018.
[28] N. T. Q. Hoa, P. H. Lam, P. D. Tung, T. S. Tuan, and H. Nguyen, "Numerical study of a wide-angle and polarization-insensitive ultrabroadband metamaterial absorber in visible and near-infrared region," *IEEE Photon. J,* vol. 11, no. 1, Feb. 2019, Art. no. 4600208.
[29] S. Jahani and Z. Jacob, "All-dielectric metamaterials," *Nature Nanotechnol.*, vol. 11, no. 1, pp. 23–36, 2016.
[30] P. Lalanne and G. M. Morris, "Antireflection behavior of silicon subwavelength periodic structures for visible light," *Nanotechnology*, vol. 8, no. 2, pp. 53–56, 1997.
[31] P. Baumeister, "Antireflection coatings with chebyshev or butterworth response: Design," *Appl. Opt.*, vol. 25, no. 24, pp. 4568–4570, 1986.
[32] F. Sepehripour, P. Karimi, and A. Khavasi, "Wideband and polarisation-independent antireflection coating using metamaterials," *IET Optoelectron,* vol. 14, no. 5, pp. 266–273, 2020.
[33] F. Defrance *et al.*, "1.6:1 bandwidth two-layer antireflection structure for silicon matched to the 190–310 GHz atmospheric window," *Appl. Opt.*, vol. 57, no. 18, pp. 5196–5209, 2018.
[34] D. R. Smith, D. C. Vier, T. Koschny, and C. M. Soukoulis, "Electromagnetic parameter retrieval from inhomogeneous metamaterials," *Phys. Rev. E - Statist. Nonlinear, Soft Matter Phys.*, vol. 71, no. 3, 2005, Art. no. 036617.
[35] P. Lalanne and M. Hutley, "The optical properties of artificial media structured at a subwavelength scale," *Encyclopedia Opt. Eng.*, pp. 62–71, 2003, Accessed: Oct. 13, 2020. [Online]. Available: https://www.yumpu.com/en/document/view/31445498/the-optical-properties-of-artificial-media-structured-at-a-
[36] T. K. Gaylord, W. E. Baird, and M. G. Moharam, "Zero-reflectivity high spatial-frequency rectangular-groove dielectric surface-relief gratings," *Appl. Opt.*, vol. 25, no. 24, pp. 4562–4567, 1986.
[37] S. J. Kim, J. Park, M. Esfandyarpour, E. F. Pecora, P. G. Kik, and M. L. Brongersma, "Superabsorbing, artificial metal films constructed from semiconductor nanoantennas," *Nano Lett,* vol. 16, no. 6, pp. 3801–3808, 2016.
[38] J. Zhu *et al.*, "Optical absorption enhancement in amorphous silicon nanowire and nanocone arrays," *Nano Lett,* vol. 9, no. 1, pp. 279–282, 2009.
[39] M. Altomare, N. T. Nguyen, and P. Schmuki, "Templated dewetting: Designing entirely self-organized platforms for photocatalysis," *Chem. Sci.*, vol. 7, no. 12, pp. 6865–6886, 2016.
[40] J. Ye and C. V. Thompson, "Templated solid-state dewetting to controllably produce complex patterns," *Adv. Mater.*, vol. 23, no. 13, pp. 1567–1571, 2011.
[41] C. V. Thompson, "Solid-state dewetting of thin films," *Annu. Rev. Mater. Res.*, vol. 42, no. 1, pp. 399–434, 2012.
[42] Z. Huang, N. Geyer, P. Werner, J. de Boor, and U. Gösele, "Metal-assisted chemical etching of silicon: A review," *Adv. Mater.*, vol. 23, no. 2, pp. 285–308, 2011.